

Low-rank approach to the computation of path integrals

Mikhail S. Litsarev^a, Ivan V. Oseledets^{a,b}

^aSkolkovo Institute of Science and Technology, Novaya St. 100, 143025 Skolkovo, Moscow Region, Russia

^bInstitute of Numerical Mathematics, Gubkina St. 8, 119333 Moscow, Russia

Abstract

We present a method for solving the reaction-diffusion equation with general potential in free space. It is based on approximation of the Feynman-Kac formula by a sequence of convolutions on sequentially diminishing grids. For computation of the convolutions we propose a fast algorithm based on the low-rank approximation of Hankel matrices. The requirements of the method hold $O(nrM \log M + nr^2M)$ flops in complexity and $O(Mr)$ elements in memory, where n is the dimension of the integral, $r \ll n$, and M is the size of mesh in one dimension. The presented technique can be generalized to the higher-order diffusion processes.

Keywords: Low-rank approximation, Feynman-Kac formula, Path integral, Multidimensional integration, Brownian motion, Pseudoskeleton approximation, Hankel matrix, Convolution

February 21, 2023

1. Introduction

Path integrals [1, 2, 3] play a dominant role in description of a wide range of problems in physics and mathematics. They are a universal and powerful tool for condensed matter and high-energy physics, theory of stochastic processes and parabolic differential equations, financial modelling, quantum chemistry and many others. Different theoretical and numerical approaches have been developed for their computation, among which the most used ones are the perturbation theory [4], the stationary phase approximation [5, 6], the functional renormalization group [7, 8], various Monte Carlo [9] and sparse grids methods [10, 11]. The interested reader can find particular details in the original reviews and books [12, 13, 14].

In this paper we focus on the one-dimensional reaction-diffusion equation with initial distribution $f(x) : \mathbb{R} \rightarrow \mathbb{R}^+$ and a constant diffusion coefficient σ

$$\begin{cases} \frac{\partial}{\partial t} u(x, t) = \sigma \frac{\partial^2}{\partial x^2} u(x, t) - V(x, t)u(x, t), & t \in [0, T], \quad x \in \mathbb{R}. \\ u(x, 0) = f(x) \end{cases} \quad (1)$$

This equation may be treated in terms of the Brownian particle motion [15, 16, 17], where the solution $u(x, t) : \mathbb{R} \times [0, T] \rightarrow \mathbb{R}^+$ is the density distribution of the particles. The potential (or the dissipation rate) $V(x, t)$ is bounded from below. We do not consider the drift term $\rho \frac{\partial}{\partial x} u(x, t)$ because it can be easily excluded by a substitution $u(x, t) \rightarrow \tilde{u}(x, t)e^{-\rho x}$ [18].

The solution can be expressed by the Feynman-Kac formula [19, 18, 20]

$$u_f(x, T) = \int_{C(x, 0; T)} f(\xi(T)) e^{-\int_0^T V(\xi(\tau), T-\tau) d\tau} \mathcal{D}_\xi, \quad (2)$$

where the integration is done over a set of all continuous paths $\xi(T) : [0, T] \rightarrow \mathbb{R}$ from the Banach space $\Xi([0, T], \mathbb{R})$ starting at $\xi(0) = x$ and stopping at arbitrary endpoints at time T . \mathcal{D}_ξ is the Wiener measure, and $\xi(t)$ is the Wiener

Email address: m.litsarev@skolkovotech.ru (Mikhail S. Litsarev)

process [21, 22]. One of the advantages of the formulation (2) is that it can be directly applied for the unbounded domain without any additional (artificial) boundary conditions.

Path integral (2) corresponding to the Wiener process is typically approximated by a *finite* multidimensional integral with the Gaussian measure (details are given in Section 2.1). The main drawback is that this integral is a high-dimensional one and its computation requires a special treatment. Several approaches has been developed to compute multidimensional integrals efficiently. The sparse grids approach [23] has been applied to the computation of path integrals in [24], but only for dimensions ≤ 100 , which sometimes is not enough. The main disadvantage of the Monte Carlo simulation is that it does not allow to achieve high accuracy.

There are several approaches based on the *separated representation* of tensors (the multidimensional functions defined on fine grids) in the *low-rank format* [25, 26, 27]. Among such methods [28] the ones based on the tensor train decomposition [29, 30, 31] and hierarchical Tucker format [32, 33, 34] are the most prominent opportunities that have to be investigated.

Our approach is based on the *low-rank approximation* of matrices used in absolutely different context. We formulate the Feynman-Kac formula as an iterative sequence of convolutions defined on grids of diminishing sizes. This is done in Section 3.2. To reduce the complexity of this computation, in Section 3.3 we find a *low-rank* basis set by applying the *cross approximation* (see Section 3.1) to a matrix constructed from the values of a one-dimensional function on a very large grid. That gives reduce of computational time and memory requirements, resulting in fast and efficient algorithm presented in Section 3.4. The numerical examples are considered in Section 4. The most interesting part is that we are able to treat non-periodic potentials without any artificial boundary conditions (Section 4.3).

2. Problem statement

2.1. Time discretization

Equation (2) corresponds to the Wiener process. A standard way to discretize the path integral is to break the time range $[0, T]$ into n intervals

$$\tau_k = k \cdot \delta t, \quad 0 \leq k \leq n, \quad n: \tau_n = T. \quad (3)$$

The average path of a Brownian particle $\xi(\tau_k)$ after k steps is defined as

$$\xi^{(k)} = \xi(\tau_k) = x + \xi_1 + \xi_2 + \dots + \xi_k, \quad (4)$$

where every random step ξ_i , $1 \leq i \leq k$, is independently taken from a normal distribution $\mathcal{N}(0, 2\sigma\delta t)$ with zero *mean* and *variance* equal to $2\sigma\delta t$. By definition, $\xi^{(0)} = x$.

Application of a suitable quadrature rule on the uniform grid (i.e., trapezoid or Simpson rules) with the weights $\{w_i\}_{i=0}^n$ to the time integration in (2) gives

$$\Lambda(T) = \int_0^T V(\xi(\tau), T - \tau) d\tau \approx \sum_{i=0}^n w_i V_i^{(n)} \delta t, \quad V_i^{(n)} \equiv V(\xi(\tau_i), \tau_{n-i}), \quad (5)$$

and transforms the exponential factor to the approximate expression

$$e^{-\Lambda(T)} \approx \prod_{i=0}^n e^{-w_i V_i^{(n)} \delta t}. \quad (6)$$

The Wiener measure, in turn, transforms to the ordinarily n -dimensional measure

$$\mathcal{D}_\xi^{(n)} = \left(\frac{\lambda}{\pi}\right)^{\frac{n}{2}} \prod_{k=1}^n e^{-\lambda \xi_k^2} d\xi_k, \quad \lambda = \frac{1}{4\sigma\delta t}, \quad (7)$$

and the problem reduces to an n -dimensional integral over the Cartesian coordinate space. Thus, we can approximate the exact solution (2) by $u^{(n)}(x, t)$

$$u(x, t) = \lim_{n \rightarrow \infty} u^{(n)}(x, t) \quad (8)$$

written in the following compact form

$$u^{(n)}(x, t) = \int_{-\infty}^{\infty} \mathcal{D}_{\xi}^{(n)} f(\xi^{(n)}) \prod_{i=0}^n e^{-w_i V_i^{(n)} \delta t}, \quad (9)$$

The integration sign here denotes an n -dimensional integration over the particle steps ξ_k , and $V_i^{(n)}$ is defined in (5). Our goal is to compute the integral (9) numerically.

3. Computational technique

3.1. Notations and basic facts

In this paper vectors are denoted by boldface lowercase letters, e.g., \mathbf{a} , matrices are denoted by boldface capital letters, e.g., \mathbf{A} . The i th element of a vector \mathbf{a} is denoted by a_i , the element (i, j) of a matrix \mathbf{A} is denoted by A_{ij} . A set of vectors \mathbf{a}_m , $m_0 \leq m \leq m_1$ is denoted by $\{\mathbf{a}_m\}_{m=m_0}^{m_1}$, and the i th element of a vector \mathbf{a}_m is denoted by a_{mi} .

Definition 1. Let vector $\mathbf{a} \in \mathbb{R}^k$ and vector $\mathbf{b} \in \mathbb{R}^m$ and $k \geq m$. We say that vector $\mathbf{c} \in \mathbb{R}^{m+k-1}$ is a *convolution* of two ordered vectors \mathbf{a} and \mathbf{b} labeled by

$$\mathbf{c} = \mathbf{a} \circ \mathbf{b}, \quad (10)$$

if it has the following components

$$c_i = \sum_{j=0}^{m-1} a_{i+j} b_j, \quad a_i = 0, \forall i : \{i \mid i < 0 \vee i \geq k\}. \quad (11)$$

The computation of the convolution can be naturally represented as a multiplication by the *Hankel matrix*.

Definition 2. We say that the *Hankel matrix* $\mathbf{A} \in \mathbb{R}^{k \times k}$ is generated by row $\mathbf{a} \in \mathbb{R}^k$ and column $\mathbf{b} \in \mathbb{R}^{k-1}$, and denote this by

$$\mathbf{A} = [\mathbf{a}, \mathbf{b}]_H, \quad (12)$$

in case, when

$$\mathbf{A} = \begin{pmatrix} a_0 & a_1 & a_2 & \cdots & a_{k-2} & a_{k-1} \\ a_1 & a_2 & a_3 & \cdots & a_{k-1} & b_0 \\ a_2 & a_3 & a_4 & \cdots & b_0 & b_1 \\ \vdots & \vdots & \vdots & \ddots & \vdots & \vdots \\ a_{k-2} & a_{k-1} & b_0 & \cdots & b_{k-4} & b_{k-3} \\ a_{k-1} & b_0 & b_1 & \cdots & b_{k-3} & b_{k-2} \end{pmatrix}, \quad (13)$$

and

$$\begin{aligned} \mathbf{a} &= (a_0, a_1, a_2, \dots, a_{k-2}, a_{k-1})^T, \\ \mathbf{b} &= (b_0, b_1, b_2, \dots, b_{k-2})^T \end{aligned} \quad (14)$$

This notation will be used for the computation of convolutions. As it can be directly verified, for $\alpha \in \mathbb{R}$

$$\alpha \cdot \mathbf{A} = [\alpha \cdot \mathbf{a}, \alpha \cdot \mathbf{b}]_H. \quad (15)$$

Definition 3. For two vectors \mathbf{a} and \mathbf{b} from (14) for the case $a_i = b_i, \forall i : 1 \leq i < k$, we will also write

$$\mathbf{a} = \begin{pmatrix} \mathbf{b} \\ a_k \end{pmatrix}. \quad (16)$$

For a matrix $\mathbf{A} \in \mathbb{R}^{n \times m}$ of rank r there exists [35, 36] a *skeleton decomposition*

$$\mathbf{A} = \mathbf{B}\hat{\mathbf{A}}^{-1}\mathbf{C}^T, \quad (17)$$

where the nonsingular $r \times r$ submatrix $\hat{\mathbf{A}}$ lies in rows $i \in \hat{I} = \{i_1, i_2, \dots, i_r\}$ and in columns $j \in \hat{J} = \{j_1, j_2, \dots, j_r\}$ of the matrix \mathbf{A} . We will denote this by $\hat{\mathbf{A}} = \mathbf{A}(\hat{I}, \hat{J})$.

$$\mathbf{B} = \mathbf{A}(I, \hat{J}), \quad \mathbf{C}^T = \mathbf{A}(\hat{I}, J), \quad I = \{1, \dots, n\}, \quad J = \{1, \dots, m\}. \quad (18)$$

Skeleton decomposition can be rewritten by the factorization of the matrices $\mathbf{B} = \mathbf{Q}_B \mathbf{R}_B$ and $\mathbf{C}^T = \mathbf{R}_C^T \mathbf{Q}_C^T$ by the *QR-decomposition*, and by further factorization of the matrix $\mathbf{R}_B \mathbf{G} \mathbf{R}_C^T = \mathbf{U}_G \mathbf{\Sigma}_G \mathbf{V}_G^T$ by the *singular value decomposition* (SVD) [37, 38], and multiplication of \mathbf{B} by $\mathbf{U}_G \mathbf{\Sigma}_G^{1/2}$ and $\mathbf{\Sigma}_G^{1/2} \mathbf{V}_C^T$ by \mathbf{C}^T correspondingly. Thus, we will use the dyadic decomposition of (17)

$$\mathbf{A} = \mathbf{B}\mathbf{C}^T, \quad A_{ij} = \sum_{q=1}^r B_{iq} C_{jq}. \quad (19)$$

To obtain decomposition (19) we use the *cross approximation* algorithm based on the concept of maximum volume submatrix introduced in [39, 40]. Our implementation of the *cross approximation* is based on [41, 42] and is available at [43]. Computation of rank r approximation requires $\mathcal{O}((n+m)r)$ evaluations of the elements and $\mathcal{O}((n+m)r^2)$ additional operations. This becomes crucial in practice, when the matrix element A_{ij} is a time-consuming function to be calculated in a point (i, j) for a finite time. Examples of low-rank approximations of multidimensional functions can be found in references [44, 45, 46, 47] and other reviews and works.

3.2. Multidimensional integration via the sequence of one-dimensional convolutions

Multidimensional integral (9) can be represented in terms of an iterative sequence of one-dimensional convolutions. Indeed, for a one-dimensional function $F_k^{(n)}(x)$, such that

$$F_k^{(n)}(x) = \sqrt{\frac{\lambda}{\pi}} \int_{-\infty}^{\infty} \Phi_{k+1}^{(n)}(x + \xi) e^{-\lambda \xi^2} d\xi, \quad x \in \mathbb{R}, \quad 1 \leq k \leq n, \quad (20)$$

where

$$\Phi_{k+1}^{(n)}(x) = F_{k+1}^{(n)}(x) e^{-w_k V(x, \tau_{n-k}) \delta t}, \quad (21)$$

and the boundary condition

$$F_{n+1}^{(n)}(x) = f(x), \quad (22)$$

the solution (9) is expressed as follows

$$u_f^{(n)}(x, T) = F_1^{(n)}(x) e^{-w_0 V(x, T) \delta t}. \quad (23)$$

The iteration starts from $k = n$ and goes down to $k = 1$. Since the function $\Phi_k^{(n)}(x)$ is bounded and the convolution (20) is with the exponentially decaying Gaussian, the lower and upper limits of the integral can be replaced by finite numbers.

$$F_k^{(n)}(x) \approx \tilde{F}_k^{(n)}(x) = \sqrt{\frac{\lambda}{\pi}} \int_{-a_x}^{a_x - h_x} \tilde{\Phi}_{k+1}^{(n)}(x + \xi) e^{-\lambda \xi^2} d\xi. \quad (24)$$

In other words, we suppose that the product $\Phi_{k+1}^{(n)}(x + \xi) e^{-\lambda \xi^2}$ rapidly decays so that a_x is large enough to approximate the integral (20) by $F_k^{(n)}(x) \approx \tilde{F}_k^{(n)}(x)$ in some norm with an error ε

$$\|F_k^{(n)}(x) - \tilde{F}_k^{(n)}(x)\| < \varepsilon. \quad (25)$$

Equation (24) has an important drawback: as soon as $F_1^{(n)}(x)$ is needed to be computed on the semi-open interval $[-a_x, a_x)$, the domain of the definition of $F_n^{(n)}(x)$ should be n -times larger $[-na_x, na_x)$ for n steps, because of the

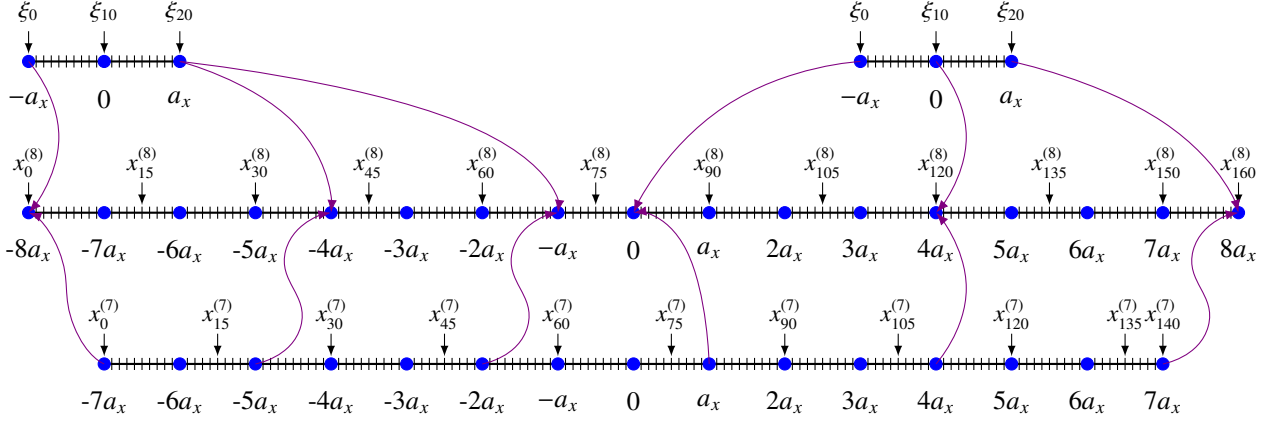


Figure 1: A correspondence of meshes for two nearest iterations $x_{i+j}^{(k+1)} = x_i^{(k)} + \xi_j$ from equation (29) for $k = 7$. Blue filled circles separate the ranges corresponding to different steps m , $1 \leq m \leq k$ in time $[-ma_x, ma_x]$. Ticks on the axis label the mesh points. Violet curved lines show correspondence (29) between two meshes for nearest iterations.

convolutional structure of the integral (24). Indeed, if we suppose, that the function $F_k^{(n)}(x)$ should be computed on the uniform mesh

$$x_i^{(k)} = -ka_x + ih_x, \quad 0 \leq i < kM, \quad h_x = a_x/N_x, \quad M = 2N_x, \quad (26)$$

and the integration mesh is chosen to be nested in (26) with the *same step* h_x

$$\xi_j = -a_x + jh_x, \quad 0 \leq j < M, \quad (27)$$

then the function $F_{k+1}^{(n)}(x)$ is defined on the mesh

$$x_i^{(k+1)} = -(k+1)a_x + ih_x, \quad 0 \leq i < (k+1)M, \quad (28)$$

and

$$x_{i+j}^{(k+1)} = x_i^{(k)} + \xi_j. \quad (29)$$

The last equality follows from definitions (26) and (27). This is illustrated in Figure 1.

The integral (24) can be calculated for every fixed $x_i^{(k)}$ of the mesh (26) as the quadrature sum with the weights $\{\mu_j\}_{j=0}^{M-1}$

$$\tilde{F}_k^{(n)}(x_i^{(k)}) \approx \sum_{j=0}^{M-1} \mu_j \tilde{\Phi}_{k+1}^{(n)}(x_{i+j}^{(k+1)}) p(\lambda, \xi_j), \quad p(\lambda, \xi) = \sqrt{\frac{\lambda}{\pi}} e^{-\lambda \xi^2} \quad (30)$$

$$\tilde{\Phi}_{k+1}^{(n)}(x_i^{(k+1)}) = \tilde{F}_{k+1}^{(n)}(x_i^{(k+1)}) e^{-w_k V(x_i^{(k+1)}, \tau_{n-k}) \delta t} \quad (31)$$

The complexity of the computation of $\tilde{F}_k^{(n)}(x_i^{(k)})$ for all i is $\mathcal{O}(kN_x^2)$ flops. It can be reduced to $\mathcal{O}(kN_x \log N_x)$ by applying the Fast Fourier transform (FFT) for convolution (30). Full computation of $\tilde{F}_1^{(n)}(x_i^{(1)})$ costs $\mathcal{O}(n^2 N_x \log N_x)$ operations and $\mathcal{O}(nN_x)$ memory. This complexity becomes prohibitive for large n (i.e., small time steps) and should be reduced. In the next section we present a fast approximate method for the calculation of $\tilde{F}_1^{(n)}(x_i^{(1)})$ in $\mathcal{O}(nrN_x \log N_x + nr^2 N_x)$ flops and $\mathcal{O}(rN_x)$ memory cost, $r \ll n$, by applying low-rank decompositions.

3.3. Low-rank basis set for convolution array

In this section we provide theoretical justification of our approach. Consider a sequence of matrices $\mathbf{A}^{(k)} \in \mathbb{R}^{kM \times kM}$ corresponding to the iterative process (30) and constructed in the following way

$$A_{ij}^{(k)} = a_{i+j}^{(k)} \equiv \tilde{\Phi}_k^{(n)}(x_{i+j}^{(k)}), \quad 0 \leq j < M, \quad 0 \leq i < kM, \quad (32)$$

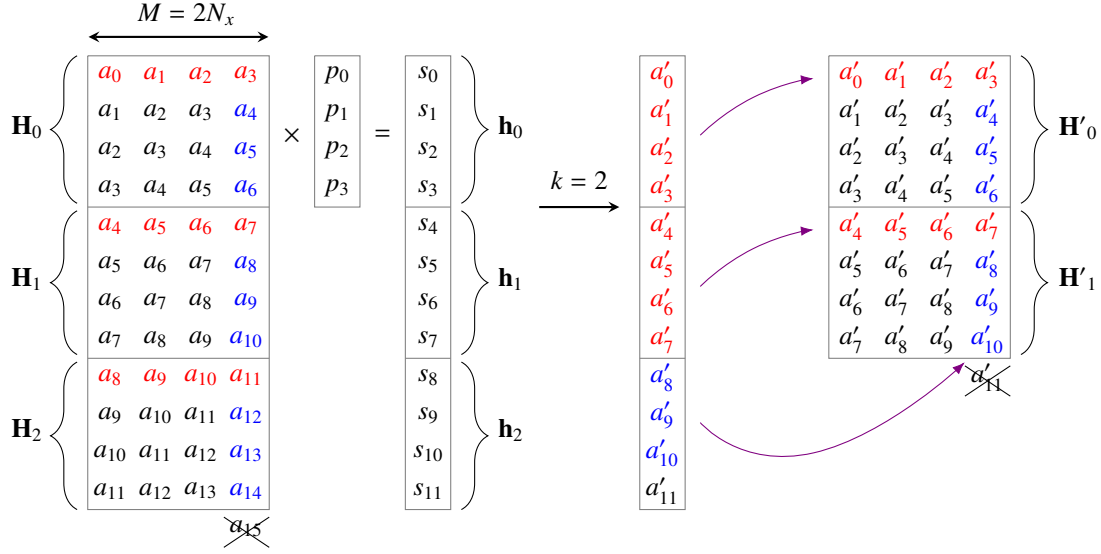


Figure 2: Transition between two neighbour iterations is illustrated. The left-hand-side matrix \mathbf{A} is multiplied by vector \mathbf{p} in a resulting vector \mathbf{s} according to (33). Explicit structure of matrix blocks \mathbf{H}_m in (34) and vector blocks \mathbf{h}_m in (38) is shown. Then entries of vector \mathbf{s} are multiplied by corresponding factor $e^{-w_k V(x_i, \tau_{n-k}) \delta t}$ to produce the next iteration step (21). From a new vector \mathbf{a}' there formed a new matrix \mathbf{A}' according to (32). The last point from the previous iteration is not needed and is thrown out. Then the steps repeat for the next iteration.

where k is the iteration number.

Let us now consider iteration (30) at the step $k = k_0$ and omit the index $k_0 + 1$ for simplicity in the matrix and mesh notations (32). Let us also denote the sum (30) for x_i taken from the grid (26) by $s_i = \tilde{F}_{k_0}^{(m)}(x_i)$ and set $p_j \equiv \mu_j p(\lambda, \xi_j)$. Then

$$s_i = \sum_{j=0}^{M-1} A_{ij} p_j \quad \Leftrightarrow \quad \mathbf{s} = \mathbf{A}\mathbf{p}. \quad (33)$$

The equality (33) establishes the correspondence between two iterations at the step k (the right-hand side) and the step $k - 1$ (the left-hand side) according to (30) and (31), see Figure 2.

The matrix \mathbf{A} is a Hankel matrix, as it follows from definition (32), and consists of k square blocks \mathbf{H}_m , $0 \leq m < k$, such that

$$\mathbf{A}^T = (\mathbf{H}_0, \mathbf{H}_1 \dots \mathbf{H}_{k-1}). \quad (34)$$

Every block \mathbf{H}_m is a Hankel matrix as well generated by the upper row \mathbf{l}_m^T and the right column \mathbf{r}_{m+1} correspondingly:

$$\mathbf{H}_m = [\mathbf{l}_m, \mathbf{r}_{m+1}]_H, \quad (35)$$

(the notation $[\mathbf{a}, \mathbf{b}]_H$ is introduced in Section 3.1, Definition 2), where

$$\begin{aligned} \mathbf{l}_m^T &= (a_{i_0}, a_{i_0+1}, \dots, a_{i_0+M-2}, a_{i_0+M-1}), \\ \mathbf{r}_m^T &= (a_{i_0}, a_{i_0+1}, \dots, a_{i_0+M-2}), \end{aligned} \quad i_0 = m \cdot M, \quad 0 \leq m < k, \quad (36)$$

by the definition, see Figure 2. It can also be represented as a sum of two anti-triangular¹ Hankel matrices

$$\mathbf{H}_m = \mathbf{L}_m + \mathbf{R}_m, \quad \mathbf{L}_m = [\mathbf{l}_{m \cdot M}, \mathbf{0}]_H, \quad \mathbf{R}_m = [\mathbf{0}, \mathbf{r}_{(m+1) \cdot M}]_H, \quad (37)$$

where the upper-left \mathbf{L}_m has nonzero anti-diagonal and the bottom-right \mathbf{R}_m has zero anti-diagonal in according to (36).

¹triangular with respect to the anti-diagonal of the matrix

Equation (33) may be rewritten in the blockwise form (see again Figure 2)

$$\mathbf{h}_m = \mathbf{H}_m \mathbf{p}, \quad \mathbf{h}_m^T = (s_{m \cdot M}, s_{m \cdot M+1} \dots s_{m \cdot M+M-1}). \quad (38)$$

Here every block \mathbf{H}_m is multiplied by the same vector \mathbf{p} . The number of matrix-vector multiplications can be reduced, if the dimension d of the linear span $\mathcal{H} = \{\mathbf{H}_m\}_{m=0}^{k-1}$ is less than k . Before estimation of the dimension we will prove some auxiliary lemmas.

Lemma 1. *Let $\{\mathbf{u}_i\}_{i=0}^{r_1-1}$ be a basis set of span $\{\mathbf{l}_m\}_{m=0}^{k-1}$, $r_1 \leq k$, and $\mathbf{U}_i = [\mathbf{u}_i, \mathbf{0}]_H$. Then $\{\mathbf{U}_i\}_{i=0}^{r_1-1}$ is a basis set of span $\{\mathbf{L}_m\}_{m=0}^{k-1}$ from (37).*

Proof. For the basis set $\{\mathbf{u}_i\}_{i=0}^{r_1-1}$ the following equality holds

$$\mathbf{l}_m = \sum_{i=0}^{r_1-1} \alpha_{mi} \mathbf{u}_i. \quad (39)$$

Then, according to (15)

$$[\mathbf{l}_m, \mathbf{0}]_H = \left[\sum_{i=0}^{r_1-1} \alpha_{mi} \mathbf{u}_i, \mathbf{0} \right]_H = \sum_{i=0}^{r_1-1} \alpha_{mi} [\mathbf{u}_i, \mathbf{0}]_H, \quad \Leftrightarrow \quad \mathbf{L}_m = \sum_{i=0}^{r_1-1} \alpha_{mi} \mathbf{U}_i, \quad \forall m \in [0, k-1]. \quad (40)$$

□

Lemma 2. *Let $\{\mathbf{w}_i\}_{i=0}^{r_2-1}$ be a basis set of span $\{\mathbf{r}_m\}_{m=1}^k$, $r_2 \leq k$, and $\mathbf{W}_i = [\mathbf{0}, \mathbf{w}_i]_H$. Then $\{\mathbf{W}_i\}_{i=0}^{r_2-1}$ is a basis set of span $\{\mathbf{R}_m\}_{m=0}^{k-1}$ from (37).*

Proof. From the equality $\mathbf{r}_m = \sum_{i=0}^{r_2-1} \beta_{mi} \mathbf{w}_i$ it follows that

$$[\mathbf{0}, \mathbf{r}_m]_H = \left[\mathbf{0}, \sum_{i=0}^{r_2-1} \beta_{mi} \mathbf{w}_i \right]_H = \sum_{i=0}^{r_2-1} \beta_{mi} [\mathbf{0}, \mathbf{w}_i]_H, \quad \Leftrightarrow \quad \mathbf{R}_m = \sum_{i=0}^{r_2-1} \beta_{mi} \mathbf{W}_i, \quad \forall m \in [0, k-1]. \quad (41)$$

□

Lemma 3. *Let $\{\mathbf{u}_i\}_{i=0}^{r_1-1}$ be a basis set of span $\{\mathbf{l}_m\}_{m=0}^k$, such that $\mathbf{u}_i^T = (\mathbf{w}_i^T, u_{i,(M-1)})$ according to (16). Then $\{\mathbf{w}_i\}_{i=0}^{r_1-1}$ is a basis set of span $\{\mathbf{r}_m\}_{m=1}^k$.*

Proof. From definition (36) and the decomposition $\mathbf{l}_m = \sum_{i=0}^{r_1-1} \gamma_{mi} \mathbf{u}_i$, $\forall j_m \in [0, k]$, it follows that

$$\begin{pmatrix} \mathbf{r}_m \\ l_{m,(M-1)} \end{pmatrix} = \mathbf{l}_m = \sum_{i=0}^{r_1-1} \gamma_{mi} \mathbf{u}_i = \sum_{i=0}^{r_1-1} \gamma_{mi} \begin{pmatrix} \mathbf{w}_i \\ u_{i,(M-1)} \end{pmatrix}, \quad \Rightarrow \quad \mathbf{r}_m = \sum_{i=0}^{r_1-1} \gamma_{mi} \mathbf{w}_i. \quad (42)$$

□

Let us define a basis set $\{\mathbf{Q}_i\}_{i=0}^{2r-1}$ as follows

$$\mathbf{Q}_i = \begin{cases} \mathbf{U}_i, & 0 \leq i < r \\ \mathbf{W}_{i-r}, & r \leq i < 2r \end{cases} \quad (43)$$

An obvious corollary of the previous Lemma is the following Theorem.

Theorem 1. *The dimension of the linear span of matrices $\{\mathbf{H}_m\}_{m=0}^{k-1}$ is equal to $2r$. Moreover, it is contained in the linear span of the matrices $\{\mathbf{Q}_i\}_{i=0}^{2r-1}$ defined in (43).*

Proof. The matrix \mathbf{H}_m can be written as a sum (37), $\mathbf{H}_m = \mathbf{L}_m + \mathbf{R}_m$. According to *Lemma 1*, the set $\{\mathbf{U}_i\}_{i=0}^{r-1}$ is a basis set of the span $\{\mathbf{L}_m\}_{m=0}^{k-1}$. By *Lemma 3*, $\{\mathbf{w}_i\}_{i=0}^{r-1}$ is a basis set of the span $\{\mathbf{r}_m\}_{m=0}^{r-1}$, and by *Lemma 2*, $\{\mathbf{W}_i\}_{i=0}^{r-1}$ is a basis set of $\{\mathbf{R}_m\}_{m=0}^{k-1}$. The subspaces $\{\mathbf{U}_i\}_{i=0}^{r-1}$ and $\{\mathbf{W}_i\}_{i=0}^{r-1}$ contain only zero matrix in common, so the dimension of the basis is $2r$. \square

Lemma 4. *Let $\{\mathbf{u}_i\}_{i=0}^{r-1}$ be a basis set of span $\{\mathbf{l}_m\}_{m=0}^k$. Then for basis matrices $\{\mathbf{Q}_i\}_{i=0}^{2r-1}$ defined in (43) the computation of the matrix-by-vector products*

$$\mathbf{k}_i = \mathbf{U}_i \mathbf{p}, \quad \mathbf{t}_i = \mathbf{W}_i \mathbf{p}, \quad (44)$$

costs $O(M \log M)$ flops for a fixed $0 \leq i < r$.

Proof. Consider a circulant matrix

$$\mathbf{G}_i = \begin{pmatrix} \mathbf{W}_i \\ \mathbf{U}_i \end{pmatrix}. \quad (45)$$

A product $\mathbf{G}_i \mathbf{p}$ is a result of the convolution $\mathbf{u}_i \circ \hat{\mathbf{p}}$, which can be done by the FFT [48, 49] procedure in $O(M \log M)$ flops for a fixed $0 \leq i < r$. The vector $\hat{\mathbf{p}} = (p_{M-1}, \dots, p_1, p_0)$ is taken in the reverse order. \square

Once the basis $\{\mathbf{Q}_i\}_{i=0}^{d-1}$ for the span of \mathcal{H} is found, the complexity of the multiplication (33) $\mathbf{A} \mathbf{p}$ can be estimated as follows.

Theorem 2. *Let the set $\{\mathbf{Q}_i\}_{i=0}^{2r-1}$ defined in (43) be a basis set of the linear span \mathcal{H} generated by the set of Hankel matrices \mathbf{H}_m defined in (34). Then the computation of any K_s elements s_i of the vector \mathbf{s} (33) costs $O(rM \log M + r^2 M)$ flops for $K_s = O(rM)$.*

Proof. Indeed, by the assumption $\mathbf{H}_m = \sum_{i=0}^{2r-1} c_{mi} \mathbf{Q}_i$ for each m , $0 \leq m < k$. The complexity of the product $\mathbf{Q}_i \mathbf{p}$, $0 \leq i < 2r$ for a fixed i is $O(M \log M)$ flops by Lemma 4. The computation of such products for all i takes $O(rM \log M)$ flops.

The vector \mathbf{h}_m , which is a subvector of \mathbf{s} , is represented via few matrix-by-vector products (44) as follows

$$\mathbf{h}_m = \mathbf{H}_m \mathbf{p} = \mathbf{L}_m \mathbf{p} + \mathbf{R}_m \mathbf{p} = \sum_{i=0}^r \alpha_{mi} \mathbf{U}_i \mathbf{p} + \beta_{mi} \mathbf{W}_i \mathbf{p} = \sum_{i=0}^r \alpha_{mi} \mathbf{k}_i + \beta_{mi} \mathbf{t}_i. \quad (46)$$

The computation of its i th component h_{mi} takes $O(r)$ flops for any m . Computation of $O(rM)$ components s_j of the vector \mathbf{s} , which are also the components of the particular vector \mathbf{h}_m (for $m = \lfloor \frac{j}{M} \rfloor$), costs, in turn, $O(r^2 M)$ flops. Finally, $O(rM \log M + r^2 M)$. \square

Remark 1. Each component of the resulting vector can be computed by the formula

$$s_j = h_{m_j l_j} = \sum_{i=0}^r \alpha_{m_j i} k_{i l_j} + \beta_{m_j i} t_{i l_j}, \quad m_j = \left\lfloor \frac{j}{M} \right\rfloor, \quad l_j = j \bmod M. \quad (47)$$

Here $k_{i l_j}$ is the l_j -th component of the vector \mathbf{k}_i and $t_{i l_j}$ is the l_j -th component of the vector \mathbf{t}_i .

Remark 2. As it follows from Lemma 3 in (46) $\alpha_{i+1, j} = \beta_{ij}$.

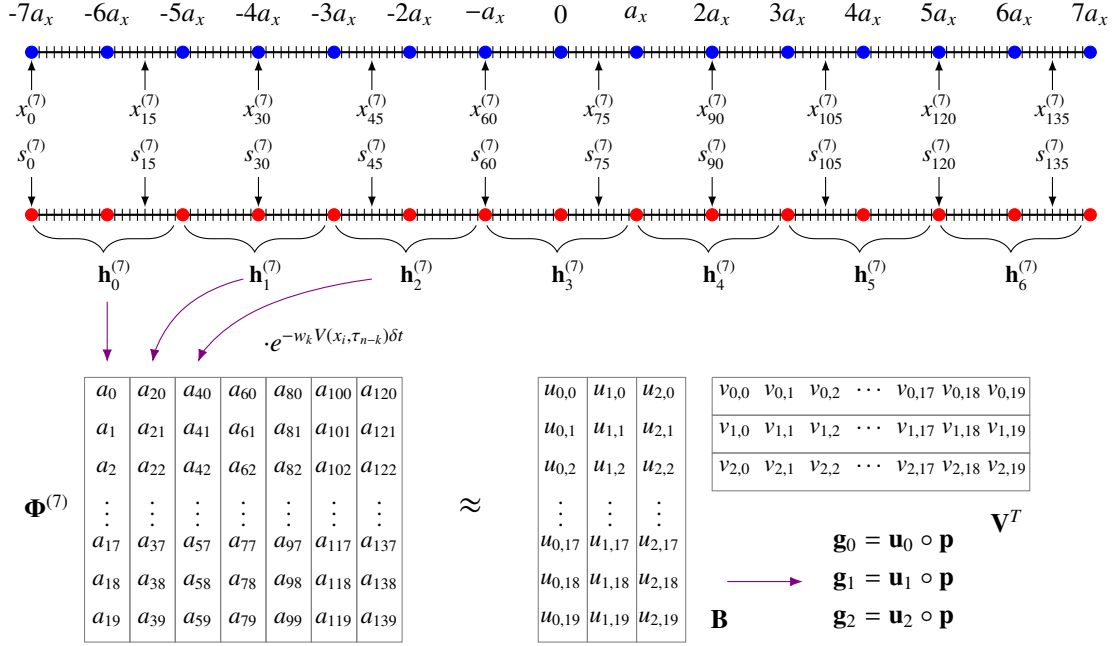


Figure 3: Construction of matrix $\Phi^{(k)}$ from a one-dimensional convolution (33) according to algorithm in Section 3.4. On a spatial homogenous mesh (26) the corresponding entries of vector \mathbf{s} (33) are calculated. By definition, vector \mathbf{s} is composed from vectors \mathbf{h}_m (38). Each column of the matrix $\Phi^{(k)}$ is composed of \mathbf{h}_m multiplied by a corresponding factor $e^{-w_k V(x_i, \tau_{n-k}) \delta t}$. Then this matrix is decomposed by a *cross approximation* $\Phi^{(k)} = \mathbf{B} \mathbf{V}$ (49). For the approximation there needed only some elements of matrix $\Phi^{(k)}$, which are chosen adaptively and computed on-a-fly. Then convolutions $\mathbf{g}_i = \mathbf{u}_i \circ \mathbf{p}$ are calculated via fast Fourier transform and saved in the memory. Particular values of $s_i^{(k)}$ for the next iteration step $k - 1$ can be computed by formula (47) then.

3.4. Final algorithm

To compute $\tilde{F}_1^{(n)}(x_i)$, which defines the final solution (23) on the mesh (26), one needs to iterate equation (30) starting from $k = n$ down to 1. At each iteration step k we construct a function $f_k(x_i^{(k)})$, which *approximates* any entry of s_i^k array according to equation (47) by the following way. Suppose, that the function $f_{k+1}(x_i^{(k+1)})$ has been already constructed for the previous step $k + 1$. Then, to compute $f_k(x_i^{(k)})$ at the current iteration k , we consider² the matrix $\Phi^{(k+1)}$ with the entries

$$\Phi_{ij}^{(k+1)} = f_{k+1}(y_{ij}) e^{-w_k V(y_{ij}, \tau_{n-k}) \delta t}, \quad y_{ij} = x_{i+j, M}^{(k+1)}, \quad (48)$$

and apply the *cross approximation* (19) to this matrix. The columns of this matrix are vectors $\mathbf{h}_m^{(k+1)}$ element-wise multiplied by the corresponding exponential factor with the potential (48), see Figure 3. The algorithm of the cross approximation requires only $\mathcal{O}(rM)$ elements, which are being chosen adaptively. They are calculated by the function $f_{k+1}(y_{ij})$ on-the-fly for the particular points y_{ij} . Thus,

$$\Phi^{(k+1)} = \mathbf{B} \mathbf{V}^T, \quad \mathbf{B} \in \mathbb{R}^{M \times r}, \quad \mathbf{V} \in \mathbb{R}^{(k+1) \times r}, \quad r \ll M. \quad (49)$$

Matrices \mathbf{B} and \mathbf{V} are saved in the memory. By construction the m -th column of matrix $\Phi^{(k+1)}$ is a vector \mathbf{l}_m from (36) and the i -th column of matrix \mathbf{B} is a basis vector \mathbf{u}_i from Lemma 1. \mathbf{V}^T is the matrix of coefficients of the decomposition (39). Once the cross approximation (49) is obtained, the memory allocated for all data structures related to $f_{k+1}(x_i^{(k+1)})$ can be deallocated or reused at the next iteration.

²but do not compute all its elements

Computation of the circulant matrix-vector products (44) is done according to Lemma 4 by the convolution $\mathbf{g}_i = \mathbf{b}_i \circ \hat{\mathbf{p}}$, where \mathbf{b}_i is a column of the matrix \mathbf{B} . The vectors $\mathbf{g}_i = (\mathbf{t}_i, \mathbf{k}_i)^T$ are also saved in memory. Then $f_k(x_i^{(k)})$ can be calculated by equation (47), and the algorithm can proceed to the next iteration.

At some step that will happen, that the rank of the decomposition (49) becomes equal to the number of columns and for further calculation it is more effective to do the convolution (33) without low-rank approximation. Complexity of one step of the presented algorithm is estimated in Theorem 2. Finally, for all n steps it is $O(nrM \log M + nr^2M)$.

4. Numerical experiments and discussions

4.1. Harmonic Oscillator

As a first example, let us consider a model system, which can be solved analytically, with the initial condition $f_{ho}(x)$ and the dissipation rate $V_{ho}(x, t)$ defined as

$$f_{ho}(x) = p(\beta, x) = \sqrt{\frac{\beta}{\pi}} e^{-\beta x^2}, \quad V_{ho}(x, t) = \frac{x^2}{t+1}. \quad (50)$$

According to equation (23) the exact solution $u_{ho}^{(n)}(x, t)$ for the particular case (50) has the following form (see Appendix A)

$$u_{ho}^{(n)}(x, t) = \Psi_1^{(n)}(x) e^{-w_0 V_{ho}(x, t) \delta t}. \quad (51)$$

Comparison of the numerical low-rank solution with the exact one (51) gives the relative error of the machine precision

$$\epsilon = \|\tilde{\mathbf{u}} - \mathbf{u}\| / \|\mathbf{u}\|, \quad (52)$$

where $\tilde{\mathbf{u}}$ is an approximate solution on the final mesh and \mathbf{u} is the exact one on the same mesh. For our example

$$\tilde{u}_i = \tilde{F}_1^{(n)}(x_i) e^{-w_0 V_{ho}(x_i, T) \delta t}, \quad u_i = \Psi_1^{(n)}(x_i) e^{-w_0 V_{ho}(x_i, T) \delta t}. \quad (53)$$

Here $\sigma = 0.25$, $T = 10$, $n = 100$, and the mesh is a uniform one on $[-2, 2]$ with $M = 2N_x = 8000$ points. It is interesting that the scheme is exact for this case.

4.2. Cauchy Distribution

The second example is taken from [24] and is interesting because it can be solved analytically as well. For $V_c(x, t)$ and initial condition $f_c(x)$ such that

$$V_c(x, t) = -\frac{1}{t+1} + 2\sigma \frac{3x^2 - 1}{(x^2 + 1)^2}, \quad f_c(x) = \frac{1}{\pi} \frac{1}{x^2 + 1}, \quad (54)$$

the exact solution is

$$u_c(x, t) = \frac{1}{\pi} \frac{t+1}{x^2 + 1}. \quad (55)$$

In Table 1 we present numerical results demonstrating the numerical order of scheme by the Runge formula

$$p = \log_2 \frac{\|\mathbf{u}_n - \mathbf{u}_{n/2}\|}{\|\mathbf{u}_{n/2} - \mathbf{u}_{n/4}\|}, \quad (56)$$

with respect to δt and the timings for the whole computation. Here \mathbf{u}_n is the computed solution at the final step in time.

Using our approach, it becomes possible to calculate $u^{(n)}(x, t)$ for large values of final time T due to the *low-rank* approximation of matrices $\Phi^{(k)}$ composed from the columns of the integrand values (see Section 3.4). That significantly reduces the computational cost. For an example, for the last row of Table 1 iterations start from the calculation of the convolution on the range $[-16386, 16386)$ with 32 772 000 mesh points. This is reduced to the calculation of 10 (the rank) convolutions of two arrays with 8000 elements.

Table 1: Convergence rate for system (54). Accuracy of the cross approximation $\varepsilon = 10^{-10}$. Direct convolutions start from $n = 20$, $\sigma = 0.5$, range of final spatial domain is $[-2, 2)$, $N_x = 4000$. Dimension of the integral (9) is labeled by n , δt is a time step, T is a final time for solution $u(x, T)$, ϵ is an error estimated by the Richardson extrapolation, and p is the order of the scheme for δt . Ranks of the matrix $\Phi^{(k)}$ from (49) are presented in column labeled by r . The time of computation of the integral (9) in *all points* of the mesh is reported in the last column.

T	n	δt	p	ϵ	r	time (min.)
1.0	32	$3.1 \cdot 10^{-2}$	–	$2.8 \cdot 10^{-4}$	10	0.1
	64	$1.6 \cdot 10^{-2}$	–	$7.0 \cdot 10^{-5}$	10	0.2
	128	$7.8 \cdot 10^{-3}$	1.997	$1.8 \cdot 10^{-5}$	10	0.4
	256	$3.9 \cdot 10^{-3}$	1.999	$4.4 \cdot 10^{-6}$	10	0.9
	512	$2.0 \cdot 10^{-3}$	2.0	$1.1 \cdot 10^{-6}$	10	1.8
	1024	$9.8 \cdot 10^{-4}$	2.0	$2.8 \cdot 10^{-7}$	10	3.8
20.0	32	$6.3 \cdot 10^{-1}$	–	$4.1 \cdot 10^{-1}$	10	0.1
	64	$3.1 \cdot 10^{-1}$	–	$1.6 \cdot 10^{-1}$	10	0.2
	128	$1.6 \cdot 10^{-1}$	1.10	$4.8 \cdot 10^{-2}$	10	0.4
	256	$7.8 \cdot 10^{-2}$	1.68	$1.2 \cdot 10^{-2}$	10	0.9
	512	$3.9 \cdot 10^{-2}$	1.93	$3.1 \cdot 10^{-3}$	10	1.9
	1024	$2.0 \cdot 10^{-2}$	1.98	$7.9 \cdot 10^{-4}$	10	4.0
	2048	$9.8 \cdot 10^{-3}$	1.995	$2.0 \cdot 10^{-4}$	10	8.0
	4096	$4.9 \cdot 10^{-3}$	1.999	$4.9 \cdot 10^{-5}$	10	16.8
	8192	$2.4 \cdot 10^{-3}$	2.0	$1.2 \cdot 10^{-5}$	10	37.5

As it can be seen from our results, the scheme has second order in time. It can be improved to higher orders by Richardson extrapolation on fine meshes [50, 51]. Another way is to use other path integral formulations with high-order propagators [52, 53].

It should be noted that the presented method needs a constant memory size, which depends only on the final mesh size M and the rank r of the matrix $\Phi^{(k)}$ from (49) at each iteration, thus it is similar to the classical time-stepping schemes for the solution of the reaction-diffusion equations in a bounded domain.

4.3. Periodic potential with impurity

The dissipation rate $V(x, t)$ causes the creation and annihilation of diffusing particles, as it follows from the main equation (1). Without the Laplacian, which is responsible for the free diffusion we have

$$\frac{\partial}{\partial t} u(x, t) = -V(x, t)u(x, t). \quad (57)$$

It can be seen, that the density of particles increases over time for $V(x, t) < 0$ and decreases for $V(x, t) > 0$ correspondingly. The cases of $V(x, t) < 0$ may lead to instability in the solution, because the integral

$$\int_{-\infty}^{\infty} f(x + \xi) e^{-w_i V(x+\xi, \tau_{n-i}) \delta t} e^{-\lambda \xi^2} d\xi, \quad (58)$$

may diverge (see Eq. (9)). Nevertheless, the potential $V(x, t)$ may be taken to be also negative for the cases the integral (58) converges.

Consider the following problem (visualised on Figure 4)

$$V_i(x) = a + \sin^2\left(\pi\left(\frac{x}{a} + 1\right)\right) - \frac{1}{1 + \left(\frac{x}{a} + 1\right)^8}, \quad f_i(x) = \sqrt{\frac{\beta}{\pi}} e^{-\beta(x-a)^2}, \quad a = 0.5, \quad \beta = 0.5. \quad (59)$$

It can be interpreted as a periodic system with an impurity. The term $V(x)$ does not decay in the spatial domain and it is not periodic. The reduction of this problem to a bounded domain is not a trivial task and would require sophisticated artificial boundary conditions.

In Table 2 we present results of numerical calculations, which show the order of the numerical scheme. In Figure 5 we also show the computed solutions for different values of n . Even in this case, the solution converges with the order $p = 2$. We also used the Richardson extrapolation of $u(x, T)$ for different n to get higher order schemes in time.

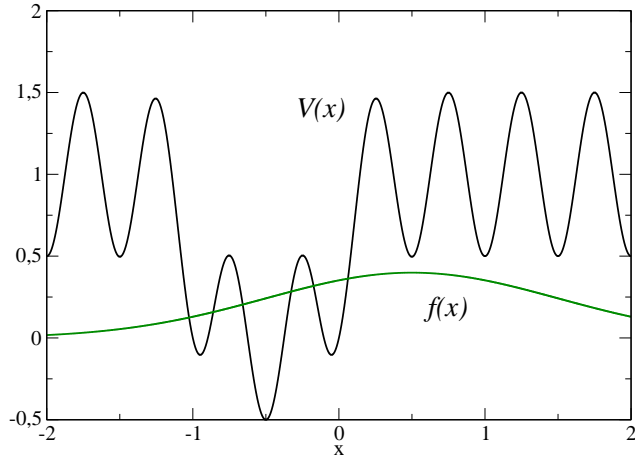


Figure 4: Potential $V(x)$ and initial distribution $f(x)$ for periodic system with impurity (59). Potential oscillates on a free space. Functions $V(x)$ and $f(x)$ are relatively shifted to break the symmetry.

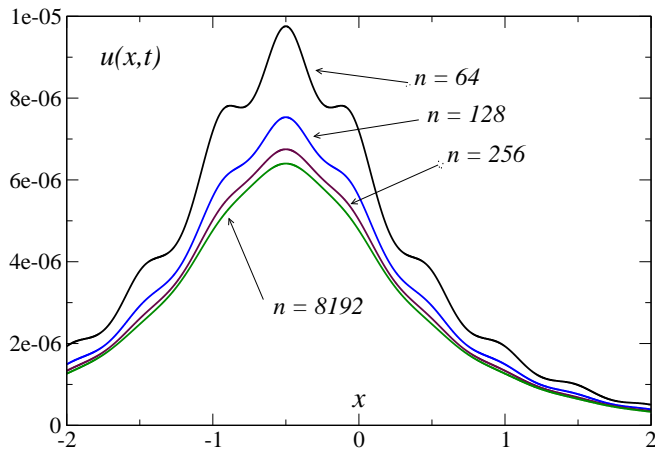


Figure 5: Convergence of solution $u(x,t)$ for periodic potential with impurity (59) for different n . This results correspond to the data presented in Table 2. The number of spacial mesh points $M = 2N_x = 8000$ in the final range $[-2, 2)$. The dissipation rate (59) leads to a decrease of the norm of the distribution density. It may be seen from the picture, that solution is far from the correct one for low dimensions $n = 64, 128, 256$.

Table 2: Convergence rate for system (59). Accuracy of the cross approximation $\varepsilon = 10^{-12}$. Direct convolutions start from $n = 20$, $\sigma = 0.25$, final domain is $[-2, 2]$, $N_x = 8000$. Dimension of the integral (9) is labeled by n , δt is the time step, $T = 20$ is the final time. The order of the scheme p_2 for δt and the relative error ε_2 (52) are estimated from the original data computed by the algorithm from Section 3.4. The next values p_4 and ε_4 are estimated by the Richardson extrapolation. As it can be seen, the scheme has the fourth order in time after the extrapolation. The ranks of the matrix $\Phi^{(k)}$ from (49) are given in the column labeled by r . The time of computation of the integral (9) in *all points* of the mesh is reported in the last column.

n	δt	p_2	ε_2	p_4	ε_4	r	time (min.)
64	$3.1 \cdot 10^{-1}$	–	–	–	–	9	0.2
128	$1.6 \cdot 10^{-1}$	–	$8.3 \cdot 10^{-2}$	–	–	9	0.3
256	$7.8 \cdot 10^{-2}$	1.47	$3.3 \cdot 10^{-2}$	–	$2.8 \cdot 10^{-3}$	9	0.8
512	$3.9 \cdot 10^{-2}$	1.62	$1.1 \cdot 10^{-2}$	2.00	$7.0 \cdot 10^{-4}$	9	1.7
1024	$2.0 \cdot 10^{-2}$	1.84	$3.1 \cdot 10^{-3}$	3.04	$8.6 \cdot 10^{-5}$	9	3.6
2048	$9.8 \cdot 10^{-3}$	1.95	$8.1 \cdot 10^{-4}$	3.66	$6.8 \cdot 10^{-6}$	9	7.0
4096	$4.9 \cdot 10^{-3}$	1.988	$2.0 \cdot 10^{-4}$	3.85	$4.7 \cdot 10^{-7}$	9	14.7
8192	$2.4 \cdot 10^{-3}$	1.997	$5.1 \cdot 10^{-5}$	3.98	$3.0 \cdot 10^{-8}$	9	33.0

4.4. Monte Carlo experiments

In this section we present results of Monte Carlo simulation. To estimate the solution in a *fixed point* x_0 the following formula is used

$$u_{MC}^{(n)}(x_0, T) = \frac{1}{K} \sum_{k=1}^K f(\xi_{(k)}(n)) \prod_{i=0}^n e^{-w_i V(\xi_{(k)}(i), \tau_{n-i}) \delta t}, \quad (60)$$

$$\xi_{(k)}(i) = \xi_{(k)1} + \dots + \xi_{(k)i}, \quad (61)$$

where each component of the vector $\xi_{(k)} = (\xi_{(k)1}, \dots, \xi_{(k)n})^T$ is independently taken from the normal distribution $\mathcal{N}(0, 2\sigma\delta t)$ at the trial step $k : 1 \leq k \leq K$, K is the number of trials.

Results for the exactly solvable model (54) are presented in Table 3. We compare accuracy and timings for Monte Carlo and low-rank calculations. It should be noticed that in the Monte Carlo approach only one point of $u(x_0, T)$ is calculated for a fixed x_0 for one simulation, while our approach allows to compute the whole array $u(x_i, T)$ on the whole mesh simultaneously. This numerical experiments have been done on a single CPU core without parallelization of the Monte Carlo algorithm just to estimate the speedup of the low-rank computation. More advanced realization such as quasi Monte Carlo methods can be used. As it can be seen, the low-rank algorithm presented in Section 3.4 is much faster.

5. Conclusion and future work

The presented results show that the proposed method is an efficient approach for solving diffusion equations in a free space without artificial boundary conditions, and it also shows favourable scaling.

It is natural to extend the approach presented in the current work to higher dimensions. Then, instead of one-dimensional convolutions we will have to work with d -dimensional convolutions, where d is the dimension of the problem. The extended domain will be $[-na, na]^d$, where n is the number of time steps (or dimension of the path integral). Thus, it is natural to represent the solution as a $(d + 1)$ -dimensional tensor of size $M \times n \times \dots \times n$. Instead of the matrix low-rank approximation, stable low-rank factorization based on tensor train decomposition [31] will be used, with the final cost estimated as the cost of the computation the convolutions on the small domain.

Finally, the most intriguing part is to apply similar techniques to the Schrödinger equation. There, the convolution is no longer a convolution with a Gaussian function, thus the problem is much more difficult and requires modifications.

The presented method can also be applied to path integrals arising in other application areas, including the financial applications. The main requirement is that the integrated function depends on the sum of variables multiplied by a separable function.

Table 3: Timings for system (54). Accuracy of the cross approximation $\varepsilon = 10^{-10}$. Direct convolutions start from $n = 30$, $\sigma = 0.5$, range of final spatial domain is $[-2, 2]$, $N_x = 4000$. Dimension of the integral (9) is labeled by n , δt is a time step, T is a final time for solution $u(x_0, T)$ computed in a fixed point x_0 . Here $x_0 = 0$, $T = 1$. The relative error $\varepsilon = |\bar{u}(x_0, T) - u(x_0, T)|/|u(x_0, T)|$ is computed in one point x_0 . Time for one point calculation is presented for Monte Carlo approach (60) and is estimated for the whole mesh array consisting of $M = 2N_x = 8000$ points (the last column). For the low-rank computation the total timings are presented as well. Monte Carlo simulation has been done with $K = 10^9$ samples. The low-rank results are labeled by LR, while the Monte Carlo results are labeled by MC.

n	δt	$u(x_0, T)$	ε	Time (1 point)	Time (total)
32	$3.1 \cdot 10^{-2}$	0.6369899_{MC}	$5.8 \cdot 10^{-4}$	40.2 min	$5.3 \cdot 10^3$ hrs (est.)
		0.6369792_{LR}	$5.6 \cdot 10^{-4}$		6 sec
64	$1.6 \cdot 10^{-2}$	0.6367165_{MC}	$1.5 \cdot 10^{-4}$	79.1 min	$1.0 \cdot 10^4$ hrs (est.)
		0.6367099_{LR}	$1.4 \cdot 10^{-4}$		13 sec
128	$7.8 \cdot 10^{-3}$	0.6366653_{MC}	$7.2 \cdot 10^{-5}$	171 min	$2.2 \cdot 10^4$ hrs (est.)
		0.6366423_{LR}	$3.5 \cdot 10^{-5}$		26 sec
256	$3.9 \cdot 10^{-3}$	0.6366388_{MC}	$3.0 \cdot 10^{-5}$	355 min	$4.7 \cdot 10^4$ hrs (est.)
		0.6366254_{LR}	$8.9 \cdot 10^{-6}$		53 sec
512	$2.0 \cdot 10^{-3}$	0.6366218_{MC}	$3.2 \cdot 10^{-6}$	705 min	$9.4 \cdot 10^4$ hrs (est.)
		0.6366212_{LR}	$2.2 \cdot 10^{-6}$		1.8 min
		0.6366198_{exact}			

Acknowledgements

This work was partially supported by Russian Science Foundation grant 14-11-00659.

Appendix A. Solution for harmonic oscillator potential

In this section we analytically integrate equations (20), (21) (22) for initial condition (50).

Let us define $F_k^{(n)}(x) \equiv \Psi_k^{(n)}(x)$ for harmonic potential (50). Starting from $k = n$,

$$\Psi_k^{(n)}(x) = \sqrt{\frac{\lambda}{\pi}} \sqrt{\frac{\beta}{\pi}} \int_{-\infty}^{\infty} e^{-\beta(x+\xi)^2} e^{-w_n(x+\xi)^2 \delta t} e^{-\lambda \xi^2} d\xi, \quad (\text{A.1})$$

and making use of the integral

$$P(\alpha, \beta, y) = \int_{-\infty}^{\infty} p(\beta, y + \xi) p(\alpha, \xi) d\xi = p\left(\frac{\alpha\beta}{\alpha+\beta}, y\right) = \sqrt{\frac{\alpha\beta}{\pi(\alpha+\beta)}} e^{-\frac{\alpha\beta}{\alpha+\beta} y^2}, \quad y \in \mathbb{R}, \quad \alpha, \beta > 0, \quad (\text{A.2})$$

where $p(\alpha, x)$ is defined in (30), we obtain that

$$\Psi_n^{(n)}(x) = \sqrt{\frac{\beta_n}{\gamma_n}} \sqrt{\frac{\beta_{n-1}}{\pi}} e^{-\beta_{n-1} x^2}, \quad \beta_{n-1} = \frac{\lambda \gamma_n}{\lambda + \gamma_n}, \quad \gamma_n = \beta_n + w_n \delta t, \quad \beta_n = \beta. \quad (\text{A.3})$$

For the next $k = n - 1$

$$\Psi_{n-1}^{(n)}(x) = \sqrt{\frac{\lambda}{\pi}} \sqrt{\frac{\beta_n}{\gamma_n}} \sqrt{\frac{\beta_{n-1}}{\pi}} \int_{-\infty}^{\infty} e^{-\beta_{n-1}(x+\xi)^2} e^{-w_{n-1} \frac{(x+\xi)^2}{1+\delta t} \delta t} e^{-\lambda \xi^2} d\xi, \quad (\text{A.4})$$

$$\Psi_{n-1}^{(n)}(x) = \sqrt{\frac{\beta_n}{\gamma_n}} \sqrt{\frac{\beta_{n-1}}{\gamma_{n-1}}} \sqrt{\frac{\beta_{n-2}}{\pi}} e^{-\beta_{n-2} x^2}, \quad \beta_{n-2} = \frac{\lambda \gamma_{n-1}}{\lambda + \gamma_{n-1}}, \quad \gamma_{n-1} = \beta_{n-1} + w_{n-1} \frac{\delta t}{1 + \delta t}. \quad (\text{A.5})$$

By induction, we can conclude, that

$$\Psi_k^{(n)}(x) = \Gamma_k^{(n)} \sqrt{\frac{\beta_{k-1}}{\pi}} e^{-\beta_{k-1} x^2}, \quad \beta_{k-1} = \frac{\lambda \gamma_k}{\lambda + \gamma_k}, \quad \gamma_k = \beta_k + w_k \frac{\delta t}{1 + (n-k)\delta t}, \quad (\text{A.6})$$

$$\Gamma_k^{(n)} = \sqrt{\frac{\beta_n}{\gamma_n}} \sqrt{\frac{\beta_{n-1}}{\gamma_{n-1}}} \cdots \sqrt{\frac{\beta_k}{\gamma_k}}, \quad 1 \leq k \leq n \quad (\text{A.7})$$

References

1. Feynman, R.P. Space-time approach to non-relativistic quantum mechanics. *Rev Mod Phys* 1948;20:367–387. URL: <http://link.aps.org/doi/10.1103/RevModPhys.20.367>. doi:10.1103/RevModPhys.20.367.
2. Feynman, R., Hibbs, A.. Quantum mechanics and path integrals. International series in pure and applied physics; McGraw-Hill; 1965.
3. Garrod, C.. Hamiltonian path-integral methods. *Rev Mod Phys* 1966;38:483–494. doi:10.1103/RevModPhys.38.483.
4. Abrikosov, A.A., Dzyaloshinskii, I., Gorkov, L.P.. Methods of quantum field theory in statistical physics. Dover; 1975. URL: <https://cds.cern.ch/record/107441>.
5. Mahan, G.. Many-Particle Physics. Physics of Solids and Liquids; Springer; 2000. URL: <http://books.google.co.uk/books?id=xzSgZ4-yyMEC>.
6. Norman Bleistein, R.A.H.. Asymptotic Expansions of Integrals. Dover Edition; 2010.
7. Zinn-Justin, J.. Quantum field theory and critical phenomena (3d edition). Clarendon Press, Oxford; 1996.
8. Polonyi, J.. Lectures on the functional renormalization group method. *Central European Journal of Physics* 2003;1(1). URL: <http://dx.doi.org/10.2478/BF02475552>. doi:10.2478/BF02475552.
9. Dick, J., Kuo, F., Peters, G., Sloan, I.. Monte Carlo and Quasi-Monte Carlo Methods. Springer; 2012. doi:10.1007/978-3-642-41095-6.
10. Holtz, M.. Sparse Grid Quadrature in High Dimensions with Applications in Finance and Insurance. 2011. doi:10.1007/978-3-642-16004-2.
11. Garcke, J., Griebel, M.. Sparse Grids and Applications. Springer; 2013. doi:10.1007/978-3-642-31703-3.
12. Wong, K.Y.. Review of feynmans path integral in quantum statistics: from the molecular schrodinger equation to kleinerts variational perturbation theory. *Communications in Computational Physics* 2014;15(4). doi:10.4208/cicp.140313.070513s.
13. Masujima, M.. Path Integral Quantization and Stochastic Quantization. Springer; 2008.
14. Kleinert, H.. Path Integrals in Quantum Mechanics, Statistics, Polymer Physics, and Financial Markets, 5th ed. World Scientific; 2009.
15. Crank, J.. The Mathematics of Diffusion. Clarendon press, Oxford; 1975.
16. Bass, R.F.. Diffusions and Elliptic Operators. Springer; 1998.
17. Chaichian, A., Demichev, A.. Path Integrals in Physics; vol. I. IoP publishing; 2001.
18. Borodin, A.N., Salminen, P.. Handbook of Brownian motion. Facts and formulae. Springer; 2002.
19. Kac, M.. On some connections between probability theory and differential and integral equations. 1951. URL: <http://projecteuclid.org/euclid.bsmmsp/1200500229>.
20. Karatzas, I., Shreve, S.E.. Brownian motion and partial differential equations. Springer; 1991.
21. Mazo, R.M.. Brownian motion. Fluctuations, Dynamics, and Applications. Clarendon Press, Oxford; 2002.
22. Nelson, E.. Dynamical Theories of Brownian motion. Princeton University Press; 2001.
23. Gerstner, T., Griebel, M.. Dimension-adaptive tensor-product quadrature. *Computing* 2003;71:65–87. doi:10.1007/s00607-003-0015-5.
24. Gerstner, T., Griebel, M.. Numerical integration using sparse grids. *Numerical Algorithms* 1998;18(3-4):209–232. URL: <http://dx.doi.org/10.1023/A%3A1019129717644>. doi:10.1023/A:1019129717644.
25. Grasedyck, L., Kressner, D., Tobler, C.. A literature survey of low-rank tensor approximation techniques. *GAMM-Mitteilungen* 2013;36(1):53–78. URL: <http://dx.doi.org/10.1002/gamm.201310004>. doi:10.1002/gamm.201310004.
26. Kolda, T.G., Bader, B.W.. Tensor decompositions and applications. *SIAM Review* 2009;51(3):455–500. doi:10.1137/07070111X.
27. Grasedyck, L., Wolfgang, H.. An introduction to hierarchical h-rank and tt-rank of tensors with examples. *Computational Methods in Applied Mathematics* 2011;11(3):291.
28. Ballani, J.. Fast evaluation of singular bem integrals based on tensor approximations. *Numerische Mathematik* 2012;121(3):433–460. URL: <http://dx.doi.org/10.1007/s00211-011-0436-6>. doi:10.1007/s00211-011-0436-6.
29. Oseledets, I.V., Tyrtshnikov, E.E.. Breaking the curse of dimensionality, or how to use SVD in many dimensions. *SIAM J Sci Comput* 2009;31(5):3744–3759. doi:10.1137/090748330.
30. Oseledets, I.V., Tyrtshnikov, E.E.. TT-cross approximation for multidimensional arrays. *Linear Algebra Appl* 2010;432(1):70–88. doi:10.1016/j.laa.2009.07.024.
31. Oseledets, I.V.. Tensor-train decomposition. *SIAM J Sci Comput* 2011;33(5):2295–2317. doi:10.1137/090752286.
32. Hackbusch, W., Kühn, S.. A new scheme for the tensor representation. *J Fourier Anal Appl* 2009;15(5):706–722. doi:10.1007/s00041-009-9094-9.
33. Grasedyck, L.. Hierarchical singular value decomposition of tensors. *SIAM J Matrix Anal Appl* 2010;31(4):2029–2054. doi:10.1137/090764189.
34. Hackbusch, W.. Tensor spaces and numerical tensor calculus. Springer-Verlag, Berlin; 2012. ISBN 978-3642280269.
35. Goreinov, S.A., Tyrtshnikov, E.E., Zamarashkin, N.L.. Pseudo-skeleton approximations of matrices. *Reports of Russian Academy of Sciences* 1995;342(2):151–152.
36. Goreinov, S.A., Tyrtshnikov, E.E., Zamarashkin, N.L.. A theory of pseudo-skeleton approximations. *Linear Algebra Appl* 1997;261:1–21. doi:10.1016/S0024-3795(96)00301-1.
37. Golub, G.H., Loan, C.F.V.. Matrix computations, 4th edition. 2012.
38. Demmel, J.W.. Applied Numerical Linear Algebra. 1997.
39. Goreinov, S.A., Tyrtshnikov, E.E.. The maximal-volume concept in approximation by low-rank matrices. *Contemporary Mathematics* 2001;280:47–51.

40. Goreinov, S.A., Zamarashkin, N.L., Tyrtshnikov, E.E.. Pseudo-skeleton approximations by matrices of maximum volume. *Mathematical Notes* 1997;62(4):515–519. doi:10.1007/BF02358985.
41. Tyrtshnikov, E.E.. Incomplete cross approximation in the mosaic-skeleton method. *Computing* 2000;64(4):367–380. doi:10.1007/s006070070031.
42. Goreinov, S.A., Oseledets, I.V., Savostyanov, D.V., Tyrtshnikov, E.E., Zamarashkin, N.L.. How to find a good submatrix. Research Report 08-10; ICM HKBU; Kowloon Tong, Hong Kong; 2008. URL: <http://www.math.hkbu.edu.hk/ICM/pdf/08-10.pdf>.
43. Litsarev, M.S., Oseledets, I.V.. cross2d c++ code: included in the deposit distribution. ??? URL: https://bitbucket.org/appl_m729/code-deposit.
44. Khoromskij, B.N.. Introduction to tensor numerical methods in scientific computing. Preprint, Lecture Notes 06-2011; University of Zürich; 2010. URL: http://www.math.uzh.ch/fileadmin/math/preprints/06_11.pdf.
45. Oseledets, I.V.. Constructive representation of functions in low-rank tensor formats. *Constr Appr* 2013;37(1):1–18. URL: <http://pub.inm.ras.ru/pub/inmras2010-04.pdf>. doi:10.1007/s00365-012-9175-x.
46. Tyrtshnikov, E.E.. Kronecker-product approximations for some function-related matrices. *Linear Algebra Appl* 2004;379:423–437. doi:10.1016/j.laa.2003.08.013.
47. Oseledets, I.V., Savostyanov, D.V., Tyrtshnikov, E.E.. Cross approximation in tensor electron density computations. *Numer Linear Algebra Appl* 2010;17(6):935–952. doi:10.1002/nla.682.
48. Brigham, E.O.. The fast Fourier transform and its applications. Prentice Hall; 1988.
49. Nussbaumer, H.J.. Fast Fourier transform and convolution algorithms. Springer; 1981.
50. Brezinski, C., Zaglia, M.R.. Extrapolation methods. Theory and practice. Elsevier; 1991.
51. Stoer, J., Bulirsch, R.. Introduction to Numerical Analysis. 3rd ed. ed.; Springer; 2002.
52. Makri, N.. Numerical path integral techniques for long time dynamics of quantum dissipative systems. *Journal of Mathematical Physics* 1995;36(5):2430–2457. doi:<http://dx.doi.org/10.1063/1.531046>.
53. Makri, N.. Blip decomposition of the path integral: Exponential acceleration of real-time calculations on quantum dissipative systems. *The Journal of Chemical Physics* 2014;141(13):134117. doi:<http://dx.doi.org/10.1063/1.4896736>.